Board-Level Optical-to-Electrical Signal Distribution at 10 Gb/s

Yin-Jung Chang, *Student Member, IEEE*, Daniel Guidotti, Lixi Wan, Thomas K. Gaylord, *Fellow, IEEE*, and Gee-Kung Chang, *Fellow, IEEE*

***Abstract*—An opto/electrical prototype for on-board optical-to-electrical signal broadcasting operating at 10 Gb/s per channel over an interconnect distance of 10 cm is demonstrated. An improved 1×4 multimode interference (MMI) splitter at 1550 nm with linearly tapered output facet is heterogeneously integrated with four p-i-n photodetectors (PDs) on a silicon (Si) bench. The Si bench itself is hybrid integrated onto an FR-4 printed-circuit board with four receiver channels. A novel fabrication/integration approach demonstrates the simultaneous alignment between the four waveguides and the four PDs during the MMI fabrication process. The entire system is fully functional at 10 Gb/s.**

***Index Terms*—Heterogeneous/hybrid integration, multimode interference (MMI), optical interconnects, polymer waveguide.**

I. Introduction

BOARD-LEVEL optical interconnects are of growing interest for boosting chip-to-chip transmission data rates that are limited by the aspect ratio of the electrical interconnects [1], the frequency-dependent dielectric loss, and the electromagnetic interference problem in multigigahertz frequency range. It is generally agreed that optical interconnects promise substantially higher bandwidth-distance product performance over electrical links for systems requiring high aggregate bandwidth and large throughput over distances. Hence, integrated parallel optical links are of interest particularly to high-performance server/computer manufactures [2]–[4]. Among these are IBM, Intel, NEC, Fujitsu, and NTT, who are taking the lead in exploring alternatives to on-board chip-to-chip digital signaling over copper lines. Recently, the 2005 edition of the International Technology Roadmap for Semiconductors calls for on-chip frequencies to reach 23 GHz by year 2014 with a corresponding 18.6-GHz off-chip signal frequency [5].

The development of manufacturable and inexpensive integration processes for the fabrication and alignment of optical lightwave circuits with optoelectronic components is of critical importance and remains a challenge. In this letter, we demonstrate, for the first time, a multimode interference (MMI)-based opto/electrical prototype having four channels, each of which operating at 10 Gb/s, for board-level clock/signal distribution. A novel optical integration process in which four waveguides and four photodetectors (PDs) are simultaneously aligned during the MMI fabrication process is used. The prototype demonstrates the enabling technology and an inexpensive integration process for bringing high-speed optical functions to the printed-circuit board (PCB).

Manuscript received April 18, 2006; revised June 16, 2006.

The authors are with the School of Electrical and Computer Engineering and Packaging Research Center, Georgia Institute of Technology, Atlanta, GA 30332 USA (e-mail: yjchang@ece.gatech.edu).

Digital Object Identifier 10.1109/LPT.2006.881219

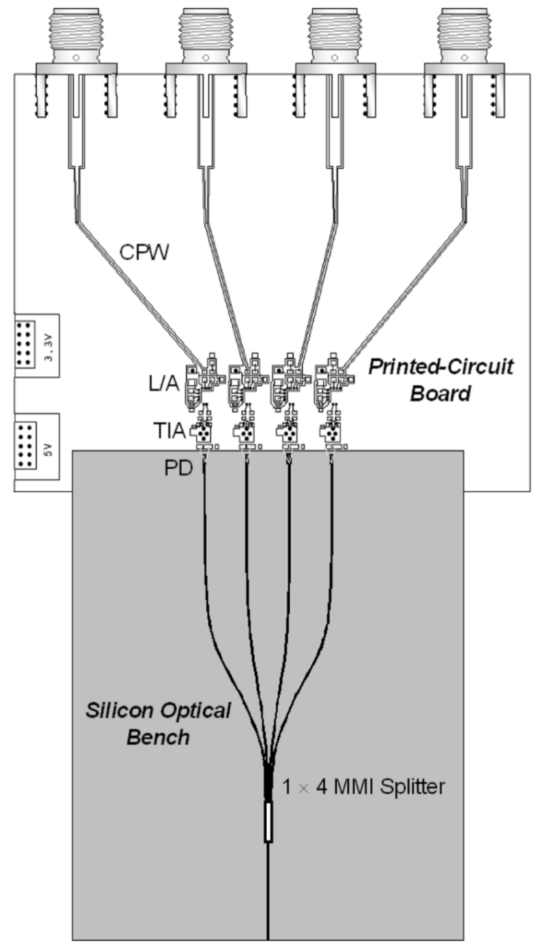

Fig. 1. Schematic of the presented optical interconnect system for board-level four-channel signal distribution at 10 Gb/s.

II. System Design

The schematic of the prototype is depicted in Fig. 1. The prototype consists of an MMI-based distribution network and four optical receivers. An MMI splitter and four PDs are fabricated and integrated on a silicon (Si) bench. For each of the four electrical channels, one transimpedance amplifier (TIA) and one limiting amplifier (L/A) along with surface-mounted capacitors and inductors are assembled on the PCB and wire bonded to the PD and circuits. The signal from the L/A is transmitted to the corresponding 3.5-mm SMA connector through coplanar waveguides for measurements.

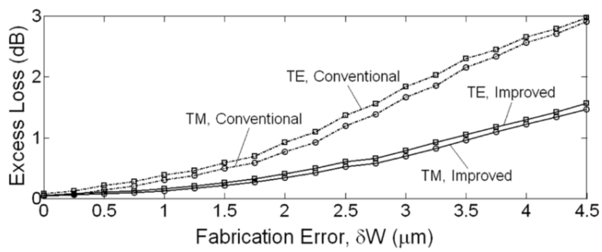

(a)

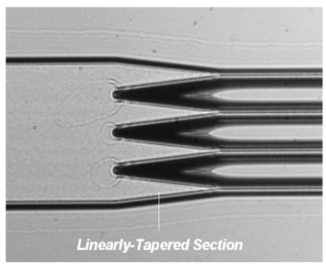

(b)

Fig. 2. Improved MMI splitter for the presented system prototype. (a) Simulated excess loss versus MMI width tolerance (δW) for the improved and conventional designs. (b) Microphotograph of the improved MMI output facet with linearly tapered sections. Input width and length of the tapered section are 60 and 180 μm, respectively. The gap between 20-μm-wide output waveguides is 40 μm. The splitter is 6.5 cm in length.

The key consideration in the system design is the optical power budget determined by the transmitter power, transmission losses, and the receiver sensitivity. Extensive effort was made to estimate and measure the various loss mechanisms. The losses are summarized as follows: a 5-dB loss introduced by the modulator due to combined modulation/insertion losses, a 0.8-dB input coupling loss at the fiber-waveguide interface, a 3.38-dB propagation loss for a 6.5-cm-long waveguide, an excess loss of 2–3 dB associated with the MMI splitter, a possible 3-dB loss at the mirror, and a 6-dB power level degradation due to four-way splitting. The power budget per channel is, thus, -5.18 dB if the continuous-wave power is 1 dBm and the receiver sensitivity is -15 dBm at 10 Gb/s. Consequently, an optical amplifier will be needed for the high-speed testing.

To increase the fabrication tolerance against the near-field diffraction due to the off-contact photolithography, the MMI structure has been improved, as shown in Fig. 2(b). Fig. 2(b) shows the microphotograph of the improved MMI output facet with linearly tapered sections. The MMI area is $L - \delta l$ in length with four tapered transitions of length δl, where L is the length of a conventional MMI splitter [6]. For a symmetric $1 \times N$ MMI splitter, the minimum sidelobe power in the vicinity of output facet occurs at transverse positions $x|_{P_{\min}} = nW/N$ with $n = \pm 1, \pm 2, \ldots \pm N/2$, where W is the width of the MMI region. Hence, the input width of the tapered section is chosen to be $W/4$. The tapered length δl is then optimized based on two-dimensional (2-D) beam propagation method (BPM) simulation. The simulated excess loss versus the fabrication tolerance of the MMI section width (δW) of the improved and conventional designs is shown in Fig. 2(a). Simulations were conducted by the 2-D BPM method with a scheme parameter of 0.54 and a mesh size of $\lambda_0/25$. For a fabrication tolerance of 4.5 μm, the excess loss of the conventional design for the TE polarization is 2.98 dB while that of the improved design is 1.57 dB. Since TM polarization has a smaller penetration depth, the excess loss of TM is smaller than that of TE. The measured excess loss among four channels ranges from 1.6 to 2.1 dB compared with a straight waveguide with the same dimensions. The discrepancy may be attributed to nonperfect sidewalls and the slight bridging at the base between adjacent tapered sections.

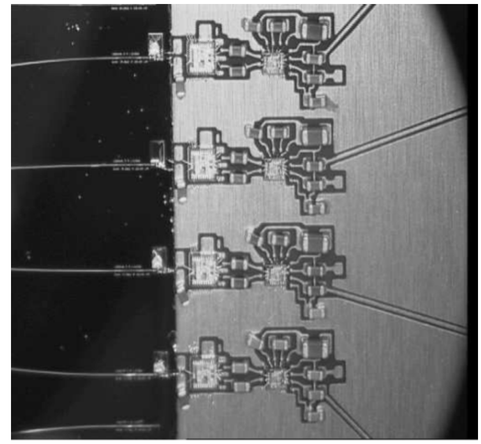

(a)

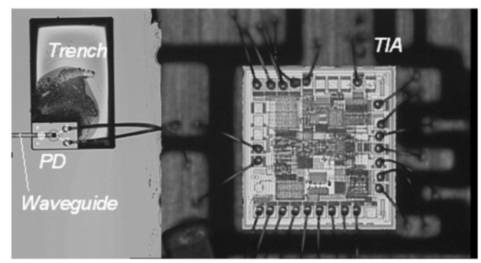

(b)

Fig. 3. (a) Panoramic view in the vicinity of optical/electrical interfaces of all channels. (b) Highlight of the output waveguide on top of the PD in the trench and a wire bonded TIA.

III. Fabrication and Integration

The optical devices were fabricated, attached, and integrated on a $\langle 100 \rangle$ Si wafer with 3-μm-thick thermal oxide. The fabrication sequences include the following steps: 1) Transfer the four trench patterns, each of which is 1.2 mm $\times$ 0.8 mm, onto a 2-μm-thick Clariant AZ 5214 photoresist whose negative reversal feature was used. 2) Remove the thermal oxide in the trench areas by a buffered oxide etchant. 3) Etch 180 $\pm$ 3 μm deep trenches with a re-entrant profile using the Bosch process. 4) Attach the PDs. 5) Fill the trenches with inorganic polymer glass (IPG) (from RPO Pty Inc.) and flood expose to UV at light. 6) Fabricate the MMI splitter using IPG and off-contact photolithography. The waveguide-PD alignment was achieved by first focusing on the active area of the PD, placing the MMI mask in near contact with the Si bench, and moving the Si bench to an optimum alignment position. 7) End mirror fabrication right atop the active areas of PDs (36 μm in diameter).

The edge effect of spin-on process produces a waveguide thickness of 37μm on top of the PDs that is favorable for the end-mirror fabrication. Each output waveguide has a linearly tapered section from 20 to 40 μm for a full coverage of the PD active area. A re-entrant trench profile is important for minimizing the gap between PDs and trench edges. Polymer filling in the trenches is used to planarize the PD-trench area and obtain

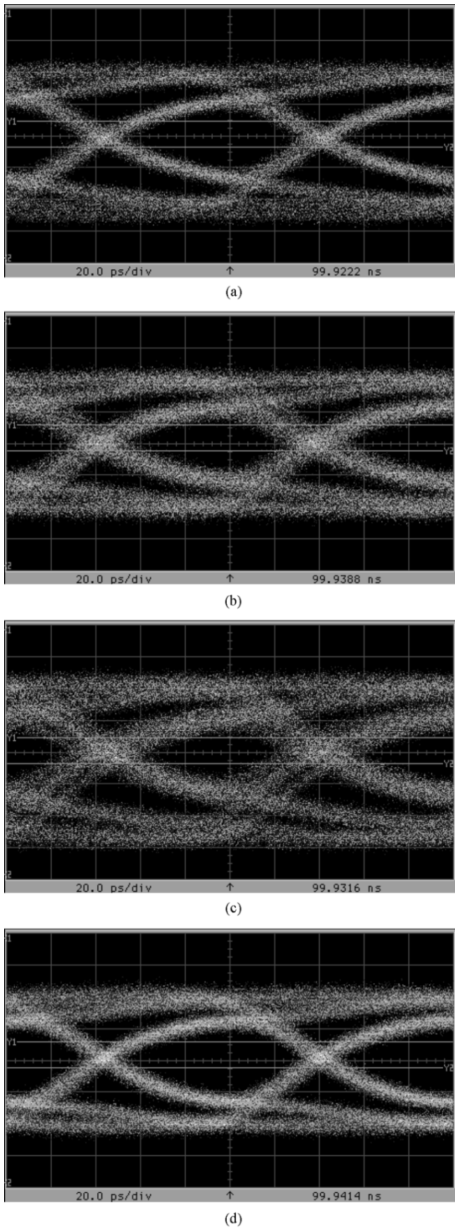

Fig. 4. Eye diagram measured from the SMA connector at (a) Channel 1, (b) Channel 2, (c) Channel 3, and (d) Channel 4 (nonreturn-to-zero format, pseudorandom binary sequence $= 2^{31} - 1$).

proper smoothness during the polymer spin-on process. Neither prebake nor postbake processes are required for the MMI fabrication. With precise control of the PD pitch, the four PDs can be simultaneously aligned to the four MMI output waveguides [Fig. 3(a)] during the MMI fabrication.

IV. Results and Discussion

There are several advantages of using different substrates for optical and electrical modules: 1) simplifying the fabrication/integration processes, 2) reducing the risks of irreversible fabrication errors, and 3) offering flexibility of replacing the defect module without rebuilding the entire system. The fabrication/integration approach mentioned above also demonstrates, for the first time, the capability of simultaneously integrating and aligning multiple polymer waveguides to multiple PDs and/or other optoelectronic devices, such as lasers, during the waveguide fabrication process.

Before the hybrid integration of the PCB with the Si bench, it is necessary to confirm each receiver channel on the PCB is fully functional. This was performed by attaching four PDs on the board and launching 10-Gb/s optical signal by direct illumination. No appreciable difference in the eye diagrams was noted between the test run and the measurement in the presence of the MMI splitter. The combined MMI excess loss and the mirror loss per channel can be measured by comparing the input power launched onto the PD (0.08 dBm) and into the MMI splitter (13.72 dBm) for obtaining a similar eye opening. It is found to be less than 3.5 dB, exclusive of a natural 6-dB power degradation. Fig. 4 gives the electrical eye diagrams measured at each channel via the corresponding SMA connector. They are all fully open and reasonably clear. The asymmetric shapes could be attributed to capacitive effects that become appreciable at 10 GHz, causing an increase in the edge rise and fall time.

V. Conclusion

An opto/electrical two-function prototype using heterogeneous/hybrid integrations for four-channel signal broadcasting at 10 Gb/s per channel was demonstrated. An interconnect distance of over 10 cm is achieved. Special designs, including an improved MMI output facet and lensless heterogeneous integration between the polymer MMI splitter and p-i-n PDs made the prototype fully functional. A radical departure from the common assembly method for the optical integration and alignment was demonstrated where the simultaneous alignment between four PDs and the four output waveguides of the 1×4 MMI splitter was achieved during the fabrication of MMI itself. The combined MMI excess loss and the mirror loss per channel is less than 3.5 dB under high-speed data transmission. The prototype demonstrates novel design/fabrication/integration technologies for the development of future high-performance opto/electrical systems.

References

[1] D. A. B. Miller and H. M. Ozaktas, "Limit to the bit-rate capacity of electrical interconnects from the aspect ratio of the system architecture," *J. Parallel Distrib. Comput.*, vol. 41, pp. 42–52, 1997.

[2] Y. S. Liu, R. J. Wojnarowski, W. A. Hennessy, and P. A. Piacente, "Plastic VCSEL array packaging and high density polymer waveguides for board and backplane optical interconnect," in *Proc. 48th IEEE Electronic Components Technology Conf.*, 1998, pp. 999–1005.

[3] Y. Ishii, N. Tanaka, T. Sakamoto, and H. Takahara, "Fully SMT-compatible optical-I/O package with microlens array interface," *J. Lightw. Technol.*, vol. 21, no. 1, pp. 275–280, Jan. 2003.

[4] J. A. Kash *et al.*, "Terabus: A chip-to-chip parallel optical interconnect," in *Proc. 18th Annu. Meeting IEEE Lasers and Electro-Optics Society (LEOS)*, 2005, pp. 363–364.

[5] International Technology Roadmap for Semiconductors 2005 Update [Online]. Available: http://public.itrs.net/

[6] L. B. Soldano and E. C. M. Pennings, "Optical multi-mode interference devices based on self-imaging: Principles and applications," *J. Lightw. Technol.*, vol. 13, no. 4, pp. 615–627, Apr. 1995.